

1 This is the peer reviewed version of the following article: Lehotai, N., Lyubenova, L.,  
2 Schröder, P., Feigl, G., Ördög, A., Szilágyi, K., Erdei, L., Kolbert, Z. (2016). Nitro-oxidative  
3 stress contributes to selenite toxicity in pea (*Pisum sativum* L). *Plant and Soil*, 400(1-2), 107-  
4 122., which has been published in final form at <http://dx.doi.org/10.1007/s11104-015-2716-x>.  
5 This article may be used for non-commercial purposes in accordance with the terms of the  
6 publisher.

7  
8

9 **Title: Nitro-oxidative stress contributes to selenite toxicity in pea (*Pisum sativum* L.)**

10 Nóra Lehotai · Lyudmila Lyubenova · Peter Schröder · Gábor Feigl · Attila Ördög · Kristóf  
11 Szilágyi · László Erdei · Zsuzsanna Kolbert

12  
13

N. Lehotai

14 UMR 1347 Agroécologie, Université de Bourgogne Franche-Comté, 17 Rue Sully, BP 86510,  
15 21065 Dijon cedex, France

16 e-mail: lehotai.nora@gmail.com · Tel: (33) 3 80 69 34 76 · Fax: (33) 3 80 69 37 53

17  
18

G. Feigl · A. Ördög · K. Szilágyi · L. Erdei · Zs. Kolbert

19 Department of Plant Biology, University of Szeged, Közép fasor 52., Szeged, Hungary

20  
21

L. Lyubenova · P. Schröder

22 Helmholtz Zentrum München, Deutsches Forschungszentrum für Gesundheit and Umwelt  
23 (GmbH), Research Unit Environmental Genomics, Ingolstaedter Landstrasse 1, D-85764  
24 Neuherberg, Germany

25  
26

**Abstract**

27 *Background and aims* Selenium (Se) phytotoxicity at the cellular level disturbs the synthesis  
28 and functions of proteins, together with the generation of an oxidative stress condition. This  
29 study reveals the nitro-oxidative stress events, supplemented by a broad spectrumed  
30 characterisation of the Se-induced symptoms.

31 *Methods* Applying several, carefully selected methods, we investigated the selenite treatment-  
32 induced changes in the Se and sulphur contents, pigment composition, hydrogen peroxide  
33 level, activity of the most important antioxidative enzymes, glutathione, nitric oxide and  
34 peroxynitrite, lipid peroxidation and protein tyrosine nitration.

35 *Results* The Se content increased intensively and concentration-dependently in the organs of  
36 the treated plants, which led to altered vegetative and reproductive development. The level of  
37 the investigated reactive oxygen species and antioxidants supported the presence of the Se-  
38 induced oxidative stress, but also pointed out nitrosative changes, in parallel.

39 *Conclusions* The presented results aim to map the altered vegetative and reproductive  
40 development of Se-treated pea plants. Mild dose of Se has supportive effect, while high  
41 concentrations inhibit growth. Behind Se toxicity, we discovered both oxidative and  
42 nitrosative stress-induced modifications. Moreover, the presented data first reveals selenite-  
43 induced concentration- and organ-dependent tyrosine nitration in pea.

44

45 **Keywords** Nitrosative stress, oxidative stress, *Pisum sativum* L., selenite

46

47

## 48 **Introduction**

49 Selenium (Se) is a non-metal microelement essential for some prokaryotes including archaea,  
50 bacteria and protozoa, certain green algae and mammals. However, the essentiality of Se in  
51 higher plants has not been proved so far (Van Hoewyk 2013). It has been described that the  
52 chemical similarity of Se to sulphur (S) makes possible its uptake and metabolism *via* S  
53 pathways in plants. Plants predominantly take up selenium by sulphate or even phosphate  
54 transporters in the form of selenate ( $\text{SeO}_4^-$ ) (Terry et al. 2000). Generally, as a naturally  
55 occurring element, Se ranges from 0.01 to 2 mg kg<sup>-1</sup> with an overall mean of 0.4 mg kg<sup>-1</sup> in  
56 soils. Elevated Se levels can also be found naturally, in soils derived from Cretaceous shale  
57 rock or as a result of anthropogenic activities, such as mining, agriculture, household or oil  
58 production (Dhillon and Dhillon 2003; Dhillon et al. 2008). Selenium levels higher than 5 mg  
59 kg<sup>-1</sup> in the tissues are toxic for most plant species (Reilly 1996). At the whole plant level, the  
60 characteristic symptoms of Se toxicity are, necrosis, withering and drying of leaves chlorosis  
61 (Mengel and Kirkby 1987), reduced photosynthetic activity and premature death (Tripathi and  
62 Misra 1974); however the toxic levels of Se for plants vary between species (Kaur et al.  
63 2014). Moreover, excess of selenium reduces shoot biomass by decreasing fresh weight,  
64 hypocotyl length and cotyledon diameter of *Arabidopsis* (Grant et al. 2011; Ohno et al. 2012;  
65 Lehotai et al. 2011) and also affects the root system through the inhibition of primary root  
66 elongation (Grant et al. 2011; Lehotai et al. 2012). At cellular level, toxicity is partly caused  
67 by the alteration of protein synthesis, structure and function, as a result of the incorporation of  
68 Se in the amino acids, cysteine and methionine. Other principle mechanism of Se

69 phytotoxicity is the disruption of the redox balance and the subsequently generated oxidative  
70 stress (Van Hoewyk et al. 2013). In the latter process, glutathione (GSH) could have a  
71 fundamental role. Its dose- and time-dependent depletion under the influence of selenium, can  
72 be the reason for growth inhibition, reactive oxygen species (ROS) production and oxidative  
73 stress, and its level has been shown to be associated with Se tolerance (Hugouvieux et al.  
74 2009; Grant et al. 2011).

75 Besides ROS, reactive nitrogen species (RNS) as the family of nitric oxide (NO)-  
76 related molecules, are also produced during diverse stress responses (Procházková et al.  
77 2014). RNS includes non-radical molecules, such as peroxynitrite (ONOO<sup>-</sup>), dinitrogen  
78 trioxide (N<sub>2</sub>O<sub>3</sub>), dinitrogen tetroxide (N<sub>2</sub>O<sub>4</sub>), *S*-nitrosoglutathione (GSNO), nitrosonium  
79 cation (NO<sup>+</sup>) and nitroxyl anion (NO<sup>-</sup>) and also radicals such as nitrogen dioxide radical  
80 (NO<sub>2</sub><sup>·</sup>) (Wang et al. 2013). The overproduction of RNS in cells results in secondary nitrosative  
81 stress (Corpas et al 2007; 2011). Since there is an active interplay between ROS and RNS and  
82 their signalling overlaps (Lindermayr and Durner 2015), the secondary stress triggered by  
83 them can be considered as nitro-oxidative stress (Corpas and Barroso 2013). An example for  
84 the ROS-RNS crosstalk is the *in vivo* formation of peroxynitrite from the reaction between  
85 superoxide anion (O<sub>2</sub><sup>-</sup>) and NO, which is responsible for the protein tyrosine nitration, a  
86 reliable biomarker of nitrosative stress in plants (Corpas et al. 2007; 2013). Tyrosine nitration  
87 is a two-step posttranslational modification process leading to a nitro group (-NO<sub>2</sub>) addition to  
88 the tyrosine radical in a radical-radical termination reaction (Souza et al. 2008). It causes  
89 steric and electronic perturbations, which modifies the tyrosine's capability to function in  
90 electron-transfer reactions or to keep the proper protein conformation (van der Vliet et al.  
91 1999). Tyrosine nitration can modify the protein functions in several ways; however the  
92 general outcome of nitration is a decreased protein activity (Corpas et al. 2013). Furthermore,  
93 tyrosine nitration can indirectly influence other signal transduction pathways e.g. by  
94 preventing the phosphorylation of tyrosine residues (Galetskiy et al. 2011).

95 Despite the importance of green pea (*Pisum sativum* L.) as a traditional edible crop  
96 cultivated in large areas and in large quantities worldwide (Santalla et al. 2001), data available  
97 on selenium accumulation and toxicity mechanisms are scarce. Moreover, considering the fact  
98 that reactive nitrogen species are multifunctional plant signals, it is attractive to hypothesize  
99 that they might be involved in selenium phytotoxicity. Therefore, the goal of this study was  
100 to characterize the accumulation and phytotoxicity of selenium in green pea, in particular the  
101 RNS-associated nitrosative processes and their crosstalk with Se-induced oxidative stress.

102

103 **Materials and methods**

104

105 **Plant material and growth conditions**

106

107 Seeds of *Pisum sativum* L. cv. Petit Provençal were surface sterilized by immersion in  
108 5% (v/v) sodium hypochlorite for 10 min, followed by washing with running water for 2 h.  
109 Germination took place in Petri dishes between moist filter papers at 26°C for 4 days.  
110 Seedlings were placed into perlite-filled plastic pots (4 seedlings/pot) and watered with full-  
111 strength Hoagland solution, resulting in semi-hydroponic conditions. Plants were  
112 precultivated for seven days and then treated with 0 (control), 10, 50 or 100 µM sodium  
113 selenite (Na<sub>2</sub>SeO<sub>3</sub>) added into the Hoagland solution for fourteen days. Plants were grown in  
114 greenhouse at a photon flux density of 150 µmol m<sup>-2</sup> s<sup>-1</sup> (12/12 h light/dark cycle) at a relative  
115 humidity of 55–60% and at 25 ± 2°C.

116 All chemicals used during the experiments were purchased from Sigma-Aldrich (St.  
117 Louis, MO, USA) unless stated otherwise.

118

119 **Element content analysis**

120

121 The element analysis was carried out with an inductively coupled plasma mass  
122 spectrometer (ICP-MS, Thermo Scientific XSeriesII, Asheville, USA). Roots and leaves of 0,  
123 10, 50 and 100 µM Se-treated pea plants were harvested separately and rinsed with distilled  
124 water. After 72 hours of drying at 70°C, nitric acid (65%, w/v) and hydrogen peroxide (H<sub>2</sub>O<sub>2</sub>,  
125 30%, w/v) (both from Reanal, Budapest, Hungary) were added to the samples, which were  
126 subjected to microwave-assisted digestion (MarsXpress CEM, Matthews, USA) at 200°C and  
127 1600 W for 15 min. Values of Se and S concentrations are given as µg g<sup>-1</sup> dry weight (DW).

128

129 **Morphological measurements**

130

131 Fresh weight (g) of the shoot and root material was measured on the 14<sup>th</sup> day of the  
132 treatment. The length (cm) of the shoot and the primary root was also measured manually  
133 using a scale. The measurements were performed by the same person to avoid human  
134 technical mistakes.

135

136 **Measurement of chlorophyll and carotenoid contents**

137

138 Total pigment content was determined according to Lichtenthaler (1987). Leaf  
139 material was homogenized in liquid nitrogen and 0.5 g of each sample was centrifuged with  
140 80% acetone for 20 min at 7000 rpm. The supernatants were collected in Falcon tubes and the  
141 pellets were subjected to a second and third repeat of the first step. The optical density (OD)  
142 was measured using a Spektral photometer (Beckman Coulter 740) at 663, 646 and 470 nm.  
143 The amount of pigments was calculated according to the equations: Chl *a* = 12.25 OD<sub>663</sub> -  
144 2.79 OD<sub>646</sub>, Chl *b* = 21.5 OD<sub>646</sub> - 5.1 OD<sub>663</sub>, Chl *a* + *b* = 7.15 OD<sub>663</sub> + 18.71 OD<sub>646</sub>, and  
145 carotenoids = (1000 OD<sub>470</sub> - 1.82 Chl *a* - 85.02 Chl *b*)/198 (Lichtenthaler 1987).

146

### 147 **Spectrophotometric determination of hydrogen peroxide**

148

149 The quantitative determination of H<sub>2</sub>O<sub>2</sub> was carried out according to the method of  
150 Velikova et al. (2000). Fresh root and leaf materials were homogenized in ice bath with 0.1%  
151 (w/v) trichloroacetic acid (TCA). After a 20 min centrifugation at 7000 rpm at 4°C,  
152 supernatants were collected and 10 mM phosphate (pH 7.0) and 1 M potassium iodide buffers  
153 were added to the samples. The absorbance was determined 10 min after the mixing step, at  
154 390 nm, using phosphate buffer as blank.

155

### 156 **Enzyme extraction**

157

158 The extraction of glutathione S-transferases (GSTs) and antioxidative enzymes was  
159 performed by the method of Schröder et al. (2005) with some modifications. Leaves and roots  
160 were homogenized in liquid nitrogen with a mortar and pestle to a fine powder and extracted  
161 at 4°C in ten-fold volumes (w/v) of 0.1 M Tris/HCl buffer (pH 7.8) containing 1% soluble  
162 PVP K90, 5 mM 1,4-dithioerythritol (DTE), 1% Nonidet P40 and 5 mM EDTA. The crude  
163 extract was centrifuged at 12 000 rpm and 4°C for 30 min. Proteins in the supernatant were  
164 precipitated by stepwise addition of solid ammonium sulfate first to 40% and then to 80%  
165 saturation. After each step, the extracts were centrifuged at 5000 rpm and 4°C for 30 min.  
166 After the second centrifugation, pellets were resuspended in 2 mL of 25 mM Tris/HCl buffer  
167 (pH 7.8), then the extracts were desalted and further purified by passing them through PD10  
168 desalting columns (Pharmacia, Freiburg, Germany). The samples were aliquoted and stored at  
169 -80°C. Concentration of proteins in the crude extract was determined according to the method

170 of Bradford (1976) using bovine serum albumin (BSA) as reference. Absorption was  
171 measured at 595 nm at room temperature.

172

### 173 **Spectrophotometric assays for antioxidative enzymes and GST determination**

174

175 Glutathione S-transferase (GST, EC 2.5.1.18) activity was assayed in standard  
176 spectrophotometric tests using different model substrates, which cover the enzyme activities  
177 of different enzyme isoforms. Aliquots of the enzyme extract were incubated with 0.1 M  
178 potassium phosphate buffer (pH 7.8), 1 mM GSH with 1 mM 1-chloro-2,4-dinitrobenzene  
179 (CDNB,  $\epsilon_{340}$  ( $\text{mM}^{-1}\text{cm}^{-1}$ )=9.6), with *p*-nitrobenzyl-chloroide (*p*-NBC,  $\epsilon_{310}$  ( $\text{mM}^{-1}\text{cm}^{-1}$ )=1.8),  
180 *p*-nitrophenylacetate (*p*-Npa,  $\epsilon_{400}$  ( $\text{mM}^{-1}\text{cm}^{-1}$ )=8.79), and with the diphenylether herbicide,  
181 fluorodifen ( $\epsilon_{400}$  ( $\text{mM}^{-1}\text{cm}^{-1}$ )=3.1).

182 Glutathione reductase (GR, EC 1.6.4.2) activity was assayed following the method of  
183 Zhang et al. (1996). Reaction mixture contained 1 mM oxidized glutathione (GSSG) and 2  
184 mM NADPH in 100 mM Tris/HCl buffer (pH 7.5) with 0.1 mM EDTA. After adding the  
185 enzyme to the mixture, the decrease of NADPH concentration through reduction of GSSG to  
186 GSH by GR ( $\epsilon_{340}$  ( $\text{mM}^{-1}\text{cm}^{-1}$ )=6.22) was determined.

187 Ascorbate peroxidase (APX, EC 1.11.1.11) was measured following the method of  
188 Vanacker et al. (1998). The reaction mixture contained 1 mM  $\text{H}_2\text{O}_2$  and 250  $\mu\text{M}$  ascorbic acid  
189 in 55.56 mM  $\text{KH}_2\text{PO}_4/\text{K}_2\text{HPO}_4$  (pH 7.0). The reaction was started by mixing the reaction  
190 mixture and the enzyme extract and the decrease of ascorbic acid concentration was recorded  
191 ( $\epsilon_{290}$  ( $\text{mM}^{-1}\text{cm}^{-1}$ )=2.8).

192 Catalase (CAT, EC 1.11.1.6) was assayed by measuring the decrease of  $\text{H}_2\text{O}_2$   
193 concentration at 240 nm by the method of Verma and Dubey (2003). The reaction mixture  
194 contained 53 mM  $\text{H}_2\text{O}_2$  in 100 mM  $\text{KH}_2\text{PO}_4/\text{K}_2\text{HPO}_4$  (pH 7.0). The buffer was mixed with  
195 the enzyme extract and the decrease of  $\text{H}_2\text{O}_2$  concentration was recorded at 240 nm ( $\epsilon_{240}$  ( $\text{mM}^{-1}\text{cm}^{-1}$ )=0.036).

197 The enzyme activity assays were carried out using a 96-well plate reader  
198 SPECTRAMax PLUS 384 spectrophotometer (Molecular Devices, Ismaning) with the data  
199 analyzing software SOFTmax PRO 4.6. The 96-well plates from Nunc (Brand, Wertheim)  
200 were applied for measuring in the visible light spectrum (390-750 nm); for assays in the UV  
201 spectrum range specific plates from Greiner (Greiner, Frickenhausen) were used. In the  
202 standard kinetic tests, absorption changes were determined in 15 sec intervals for 5 min at  
203 room temperature. The samples were measured using three technical replicates. Reaction

204 mixtures without enzyme extract were used as blanks; and enzyme activities are expressed as  
205  $\mu\text{kat mg protein}^{-1}$ . One kat represents the enzymatic formation of 1 mol end product per  
206 second in the extract.

207

208

209

210

### 211 **Quantification of total glutathione**

212

213 The measurement of total glutathione content was carried out after Griffith (1980),  
214 with some modifications. This method is based on an enzymatic recyclization through the  
215 glutathione reductase. During the reaction, the formation rate of 5-thio-2-nitrobenzoate is  
216 directly proportional to the rate of recyclization of the reaction, which is directly proportional  
217 to the GSH content. The absorbance was determined at 405 nm, using a KONTRON Uvikon  
218 Double-Beam spectrophotometer. Changes in absorbance during 1 min correspond to the  
219 concentration of GSH, using GSSG as standard.

220

### 221 **Microscopic detection of reactive oxygen and nitrogen species and glutathione**

222

223 *In situ* detection of  $\text{H}_2\text{O}_2$  in the pea leaves was carried out by using 3,3'-  
224 diaminobenzidine (DAB) staining (Guan et al. 2009). Whole leaves were incubated for 1 h in  
225 DAB solution ( $2 \text{ mg L}^{-1}$ ) on a rotary shaker (40 rpm) in the dark at room temperature.  
226 Samples were washed once with 2-N-morpholine-ethansulphonic acid/potassium chloride  
227 (MES/KCl) buffer (10/50 mM, pH 6.15).

228 The levels of nitric oxide in leaf discs and root tips were detected by 4-amino-5-  
229 methylamino- 2',7'-difluorofluorescein diacetate (DAF-FM DA) (Kolbert et al. 2012).  
230 Samples were incubated for 30 min in the dark at room temperature in  $10 \mu\text{M}$  dye solution,  
231 and were washed twice with Tris/HCl buffer (10 mM, pH 7.4).

232 The fluorophore, 3'-(p-aminophenyl) fluorescein (APF) was applied for the  
233 visualization of peroxynitrite level in the root tips and leaf discs of pea (Kolbert et al. 2012).  
234 Samples were incubated in the dark in  $10 \mu\text{M}$  dye solution for 1 hour and were washed twice  
235 with 10 mM Tris/HCl buffer.

236 Cellular glutathione levels were visualized *in situ* in the root tips with the help of  
237 monobromobimane (MBB) fluorescent staining. The root tips were incubated for 1 hour at

238 room temperature in 100  $\mu$ M dye solution (prepared in distilled water), then washed once with  
239 distilled water. For control, root tips were pre-incubated in distilled water, while as positive  
240 control, root tips were kept in 1 mM GSH solution for 20 minutes before staining. As a  
241 negative control, samples were pre-treated with 10 mM CDNB for 10 minutes.

242 Microscopic investigation of pea samples dyed with different fluorophores was  
243 performed under a Zeiss Axiovert 200M inverted microscope (Carl Zeiss, Jena, Germany)  
244 equipped with a high resolution digital camera (AxiocamHR, HQ CCD, Carl Zeiss, Jena,  
245 Germany). Filter set 10 (exc.: 450–490, em.: 515–565 nm) was used for DAF-FM and APF  
246 and filter set 49 (exc.: 365 nm, em.: 445/50 nm) was applied for MBB. Fluorescence intensity  
247 (pixel intensity) was measured on digital images using Axiovision Rel. 4.8 software, within  
248 circles of 100  $\mu$ m radii within the root tip, and of 500  $\mu$ m radii in leaf discs. Whole leaves  
249 stained with the non-fluorescent DAB were examined using Zeiss Axioscope 2000-C  
250 stereomicroscope (Carl Zeiss, Jena, Germany).

251

#### 252 **Determination of lipid peroxidation**

253

254 The level of membrane lipid peroxidation in the root and leaf tissues was quantified by  
255 measuring thiobarbituric acid reactive substances (TBARS) concentration according to the  
256 method of Heath and Packer (1968). Freshly grounded shoot and root tissues of pea were  
257 centrifuged at 10 000 rpm for 5 min in 0.1% tri-chloro acetic acid (TCA). The supernatant  
258 was removed and incubated at 95°C for 30 min in 0.5% 2-thiobarbituric acid (TBA) dissolved  
259 in 20% TCA. After cooling the samples on ice, a second centrifugation was applied at 5 000  
260 rpm for 5 min. The absorbance of the supernatant was determined at 440 nm and 532 nm, and  
261 corrected for unspecific turbidity after subtraction from the value obtained at 600 nm. The  
262 level of lipid peroxidation is expressed as  $\mu$ mol TBARS per gramm fresh weight, using an  
263 extinction coefficient of 155  $\text{mM}^{-1}\text{cm}^{-1}$ .

264

#### 265 **Immuno-detection of nitrotyrosine**

266

267 Crude protein extracts from plant material were subjected to sodium dodecyl sulphate-  
268 polyacrylamide gel electrophoresis (SDS-PAGE) on 12% acrylamide gels. For Western blot  
269 analysis, proteins were transferred to PVDF membranes using the wet blotting procedure  
270 (Bio-Rad, Hercules, CA, USA). After the transfer, membranes were blocked for 1 h with 5%  
271 non-fat milk in TBS-Tween (50 mM Tris-HCl; pH 7.4, 150 mM NaCl and 0.1% Tween-20),



272 prior used for cross-reactivity assays with rabbit polyclonal antibody against 3-nitrotyrosine  
 273 diluted 1:2000 (Corpas et al. 2008). Immuno-detection was performed by using affinity  
 274 isolated goat anti-rabbit IgG-alkaline phosphatase secondary antibody in dilution of 1:10 000,  
 275 and bands were visualised by using NBT/BCIP reaction. As a positive control nitrated bovine  
 276 serum albumin was used.

277

## 278 **Statistical analysis**

279

280 The results are expressed as mean±SE. Multiple comparison analyses were performed  
 281 with SigmaStat 12 software using analysis of variance (ANOVA,  $P \leq 0.05$ ) and Duncan's test.  
 282 In some cases, Microsoft Excel 2010 and Student's t-test were used ( $*P \leq 0.05$ ,  $**P \leq 0.01$ ,  
 283  $***P \leq 0.001$ ). All experiments were carried out at least two times. In each treatment at least 5  
 284 samples were measured.

285

286

## 287 **RESULTS**

### 288 **Selenium accumulation and translocation in green pea**

289 As an effect of the increasing external selenite concentrations, the selenium content of  
 290 the root system increased dramatically and in a concentration-dependent manner (Table 1).  
 291 Insomuch, 100  $\mu\text{M}$  sodium selenite resulted in ~1500-fold increase in Se content of the root  
 292 system, while in the leaves ~100-fold enhancement was measured. Selenium distribution,  
 293 expressed as leaf:root ratios, notably decreased as the effect of increasing treatment doses.  
 294 Sulphur concentrations were significantly increased by all selenium treatments in both organs,  
 295 compared to the controls (Table 1). However, the effect of selenite on S contents did not  
 296 prove to be concentration-dependent.

297

298 **Table 1** Total selenium (Se) and sulphur (S) concentrations ( $\mu\text{g/g}$  dry weight) in the leaves and roots of pea  
 299 plants treated with 0, 10, 50 or 100  $\mu\text{M}$  selenite. Leaf:root ratios of Se concentrations in control and selenite-  
 300 treated pea plants. Different letters indicate significant differences according to Duncan's test ( $n=6$ ,  $P \leq 0.05$ )

Na <sub>2</sub> SeO <sub>3</sub> ( $\mu\text{M}$ )	Se ( $\mu\text{g/g}$ dry weight)			S ( $\mu\text{g/g}$ dry weight)	
	leaf	root	leaf:root ratio	leaf	root
0	0.97 ± 0.06 <sup>e</sup>	0.92 ± 0.10 <sup>e</sup>	1.05	59516.66 ± 7044.72 <sup>b</sup>	50400.00 ± 5134.93 <sup>b</sup>

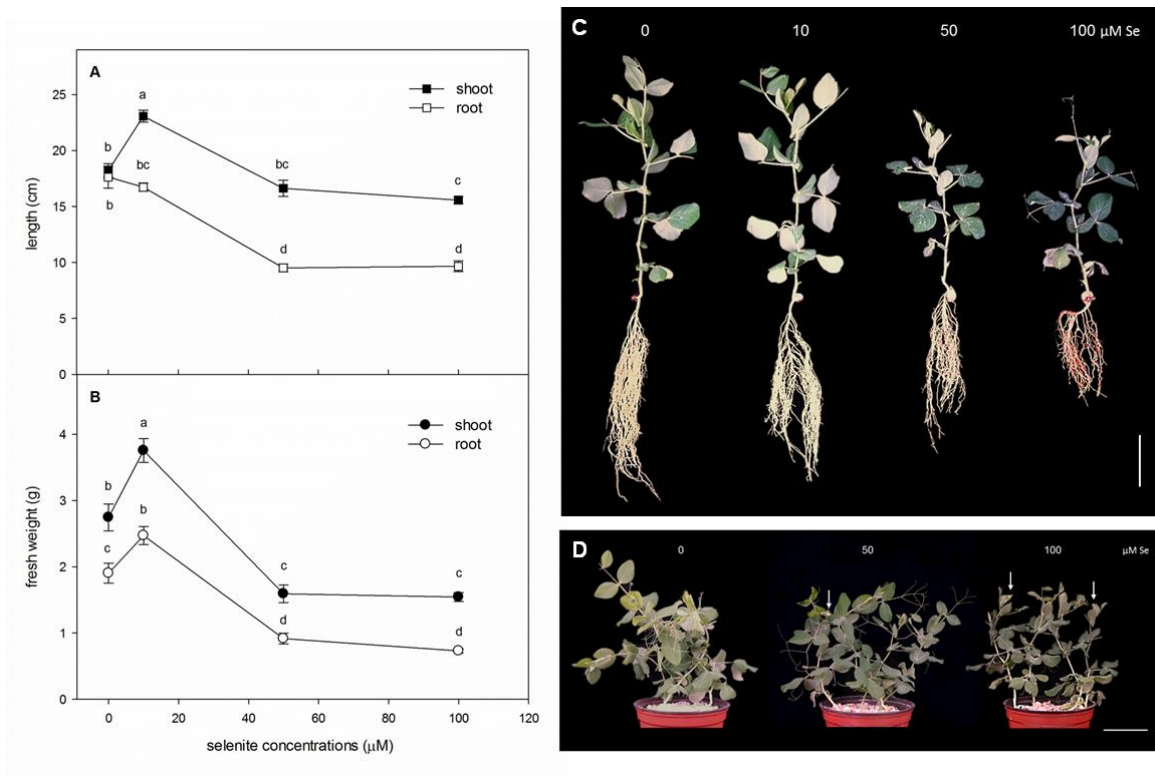
10	74.66 ± 4.41 <sup>de</sup>	303.70 ± 23.03 <sup>c</sup>	0.24	79426.66 ± 9636.44 <sup>a</sup>	76343.33 ± 12069.20 <sup>a</sup>
50	104.60 ± 3.65 <sup>d</sup>	1112.00 ± 113.92 <sup>b</sup>	0.09	68060.00 ± 9331.08 <sup>ab</sup>	78370.00 ± 11387.27 <sup>a</sup>
100	123.36 ± 8.35 <sup>d</sup>	1480.00 ± 113.92 <sup>a</sup>	0.08	75236.66 ± 8821.39 <sup>a</sup>	78586.66 ± 17827.59 <sup>a</sup>

301

## 302 Selenite altered vegetative and reproductive development of pea

303 The high amount of selenium accumulated from the external medium caused  
 304 alterations in both growth and morphology of pea plants (Fig. 1). As the effect of 10  $\mu\text{M}$   
 305 selenite, the length and the fresh weight of the shoot system significantly increased.  
 306 Regarding the roots, the elongation of the primary root slightly decreased, while the fresh  
 307 weight of the whole root system increased under the lowest selenite concentration. The more  
 308 severe Se doses (50 and 100  $\mu\text{M}$  selenite) resulted in the reduction of the shoot, root size and  
 309 fresh weight. Furthermore, these concentrations of selenite induced the premature  
 310 development of flowers (see arrows in Fig. 1D).

311



312

313 **Fig. 1** The length (cm, A) and the fresh weight (g, B) of the shoot and root system of pea plants treated with 0,  
 314 10, 50, 100  $\mu\text{M}$  selenite. Different letters indicate significant differences according to Duncan's test ( $n=6$ ,

315  $P \leq 0.05$ ). (C) Representative photographs showing the shoot and root system of control (0  $\mu\text{M}$  Se) and Se-treated  
 316 pea plants. Bar=5 cm. (D) Representative photographs showing the shoot system of control (0  $\mu\text{M}$  Se), 50 or 100  
 317  $\mu\text{M}$  Se-exposed pea. White arrows indicate flowers appeared as the effect of the treatments. Bar=10 cm

318

319 As a reliable marker for stress endurance, the photosynthetic pigment composition of  
 320 selenite-exposed pea leaves was also analysed. Excess selenium moderately decreased  
 321 chlorophyll (chl) *a* and carotenoid contents, while chl *b* concentrations showed slighter  
 322 diminution. However, in case of chlorophylls, the negative effect proved to be independent  
 323 from the applied selenite concentrations (Table 2). In general, selenium induced only slight  
 324 changes in the contents of photosynthetic pigments.

325

326

327 **Table 2** Concentrations of photosynthetic pigments ( $\mu\text{g/g}$  fresh weight) and the chlorophyll *a/b* ratios in the  
 328 leaves of control and selenite-treated pea plants. Different letters indicate significant differences according to  
 329 Duncan's test ( $n=6$ ,  $P \leq 0.05$ )

$\text{Na}_2\text{SeO}_3$ ( $\mu\text{M}$ )	Chl <i>a</i>	Chl <i>b</i>	Chl <i>a/b</i>	Total chlorophyll	Total carotenoids
0	13.37 $\pm$ 0.0115 <sup>a</sup>	3.83 $\pm$ 0.0027 <sup>b</sup>	3.48 $\pm$ 0.0041 <sup>a</sup>	17.21 $\pm$ 0.0136 <sup>a</sup>	3.44 $\pm$ 0.0030 <sup>a</sup>
10	11.82 $\pm$ 0.0052 <sup>c</sup>	3.50 $\pm$ 0.0071 <sup>c</sup>	3.37 $\pm$ 0.0112 <sup>b</sup>	15.32 $\pm$ 0.0120 <sup>c</sup>	3.28 $\pm$ 0.0026 <sup>b</sup>
50	12.28 $\pm$ 0.0049 <sup>b</sup>	4.00 $\pm$ 0.0107 <sup>a</sup>	3.06 $\pm$ 0.0140 <sup>c</sup>	16.29 $\pm$ 0.0155 <sup>b</sup>	3.23 $\pm$ 0.0062 <sup>c</sup>
100	11.36 $\pm$ 0.0048 <sup>d</sup>	3.84 $\pm$ 0.0050 <sup>b</sup>	2.95 $\pm$ 0.0081 <sup>d</sup>	15.21 $\pm$ 0.0070 <sup>d</sup>	2.95 $\pm$ 0.0018 <sup>d</sup>

330

331

332

### 333 Selenite induced oxidative stress in a concentration-dependent manner

334

335 Selenite-induced oxidative stress was characterized by measuring the  $\text{H}_2\text{O}_2$  content,  
 336 the activity of antioxidant enzymes (ascorbate peroxidase, catalase) and the accumulation of  
 337 TBARS reflecting to lipid peroxidation, which is a steady indicator for oxidative damage  
 338 (Corpas et al. 2013). Moreover, glutathione and related enzymes were also examined in the  
 339 selenite-exposed pea.

340

341

342

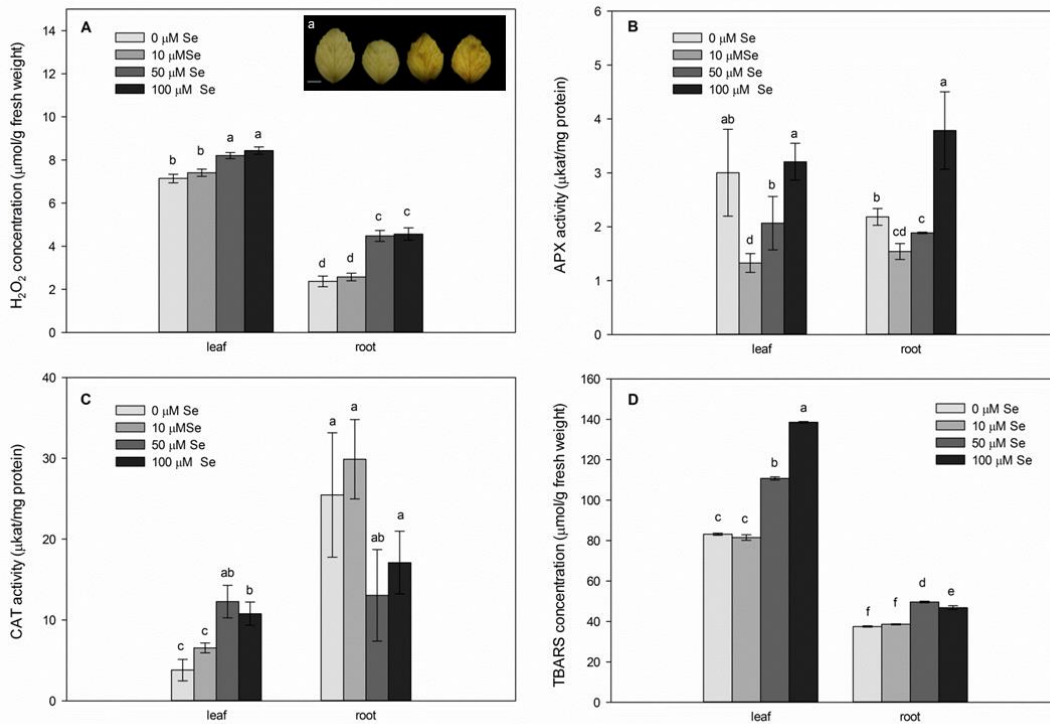
343

344

345

In both organs, the concentration of  $\text{H}_2\text{O}_2$  was increased by 50 and 100  $\mu\text{M}$  selenite,  
 but it did not show changes in case of 10  $\mu\text{M}$  Se treatment (Fig. 2A). In the leaves, the 50 and  
 100  $\mu\text{M}$  selenite-induced  $\text{H}_2\text{O}_2$  accumulation was less pronounced, however it was confirmed  
 by the intensification of brown colorization during histochemical DAB staining (Fig. 2a). The  
 specific activity of APX slightly decreased under lower selenite doses in both organs;  
 although 100  $\mu\text{M}$  Se caused an induction of the enzyme within the root system (Fig. 2B). As

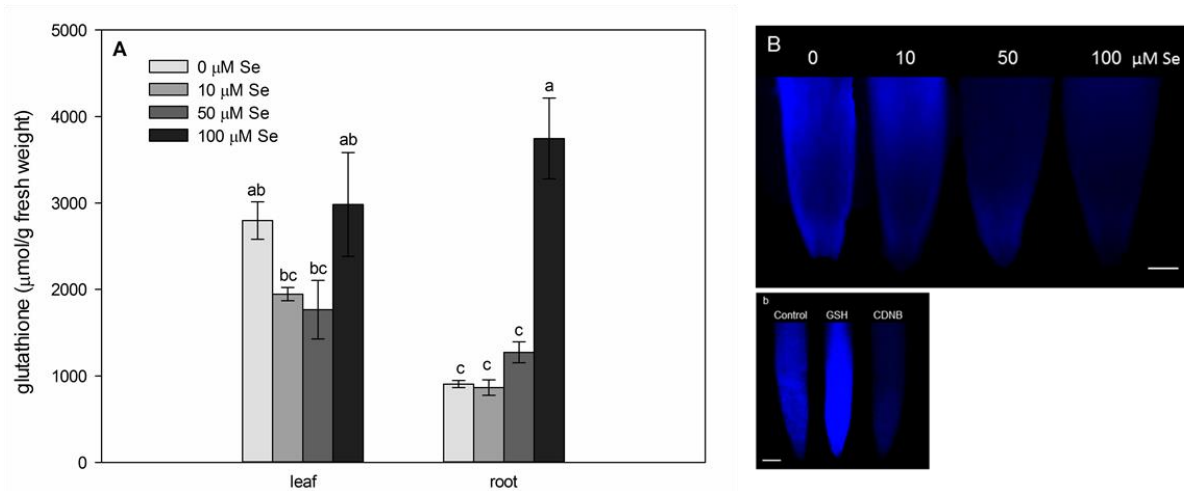
346 the effect of 50 and 100  $\mu\text{M}$  selenite, the CAT activities showed enhancement in the leaves  
 347 but reduction in the roots however, this did not prove to be significant, while 10  $\mu\text{M}$  Se did  
 348 not cause alterations in the activity of this enzyme (Fig. 2C). According to the TBARS  
 349 content, remarkable increase was observed in the leaves and minor in the roots of pea treated  
 350 with higher selenite doses (50 and 100  $\mu\text{M}$ , Fig. 2D).



351  
 352 **Fig. 2** Hydrogen peroxide concentration in pea leaves and roots, measured spectrophotometrically (A) and  
 353 detected by DAB staining (a) in the leaves of pea (from left: control, 10, 50 and 100  $\mu\text{M}$  Se, Bar=1 cm). Activity  
 354 ( $\mu\text{kat/mg}$  protein) of ascorbate peroxidase (B) and catalase (C) in the roots and leaves of pea. (D) The  
 355 concentration of TBARS in the leaf and root of pea plants treated with 0, 10, 50, 100  $\mu\text{M}$  selenite. Different  
 356 letters indicate significant differences according to Duncan's test ( $n=6$ ,  $P\leq 0.05$ )

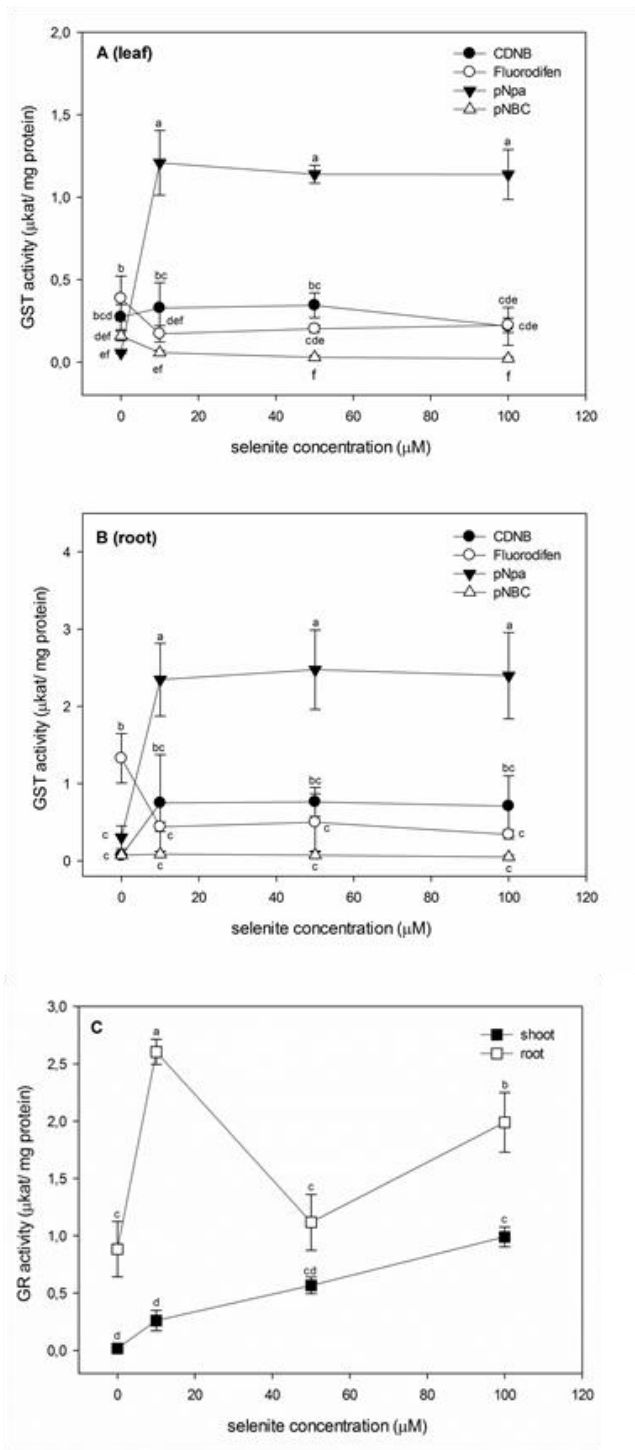
357  
 358  
 359 The glutathione concentration in the leaves was decreased after treatment with 10 and  
 360 50  $\mu\text{M}$  selenite compared to the untreated samples, while it was in the range of the control in  
 361 case of the highest Se dose. It has to be mentioned, that the changes of leaf glutathione  
 362 contents did not prove to be statistically significant (Fig. 3A). In the whole root system, the  
 363 total GSH concentration was not affected by milder selenite treatments; however it  
 364 exceptionally elevated as the effect of severe Se exposure. In contrast, within the root tips, the  
 365 intensity of the GSH-associated MBB fluorescence decreased depending on the elevating Se

366 concentrations (Fig. 3B). The GSH-dependence of the MBB fluorophore was verified by  
 367 exogenous GSH and CDNB pre-treatments (Fig. 3b).



368  
 369 **Fig. 3** (A) Concentration of total glutathione ( $\mu\text{mol/g}$  fresh weight) in the leaves and roots of control and  
 370 selenite-exposed pea. Different letters indicate significant differences according to Duncan's test ( $n=6$ ,  $P\leq 0.05$ ).  
 371 (B) Representative microscopic images of MBB-stained root tips of control ( $0 \mu\text{M Se}$ ) and 10, 50, 100  $\mu\text{M}$   
 372 selenite-treated pea. Bar= $100 \mu\text{m}$ . (b) Representative microscopic images of MBB-stained root tips treated with  
 373 water (Control), 1 mM GSH or 10 mM CDNB. Bar= $100 \mu\text{m}$

374  
 375 Selenite exposure affected the activity of GSH-associated enzymes as well. In extracts  
 376 from both roots and leaves, GST activity was assayed by using model substrates CDNB,  
 377 pNBC, fluorodifen and pNpa (Fig. 4AB). In general, the root extracts showed higher GST  
 378 activity compared to the leaf extracts and in both organs, the model substrate pNpa was  
 379 conjugated at high rates, irrespective of the Se-concentration applied. All treatments caused a  
 380 significant induction of the pNpa-GST activity independently from the concentration of  
 381 applied Se. In contrast, GST activity for the model substrate Fluorodifen notably decreased in  
 382 the leaves and roots of selenite-exposed pea. Also, glutathione reductase activity was higher in  
 383 the root system than in the leaf (Fig. 4C). In the root, selenium at low dose caused the largest  
 384 induction of the GR activity, but 50  $\mu\text{M}$  selenite did not affect it. Moreover, the 100  $\mu\text{M Se}$   
 385 concentration resulted in a moderate elevation of GR activity. In the leaves, selenite  
 386 concentration-dependently increased the GR activity; however the effect proved to be  
 387 statistically significant only in the 100  $\mu\text{M}$  selenite-treated sample.



388

389 **Fig. 4** Specific activity ( $\mu\text{kat/mg protein}$ ) of glutathione-S-transferase in control and 10, 50 or 100  $\mu\text{M}$  selenite-  
 390 treated pea leaves (A) and root (B) determined by using the model substrates CDNB, fluorodifen, pNpa and  
 391 NBC. (C) Specific activity ( $\mu\text{kat/mg protein}$ ) of glutathione reductase in the leaves and roots of pea treated with  
 392 0, 10, 50 or 100  $\mu\text{M}$  Se. Different letters indicate significant differences according to Duncan's test ( $n=5$ ,  
 393  $P \leq 0.05$ )

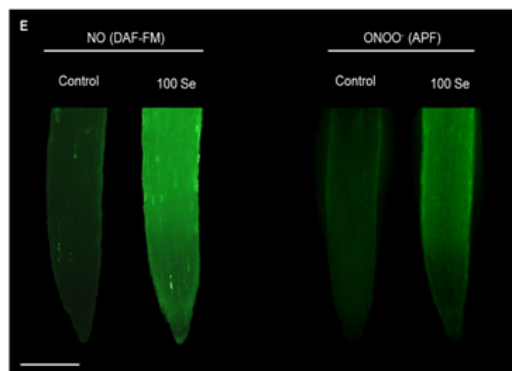
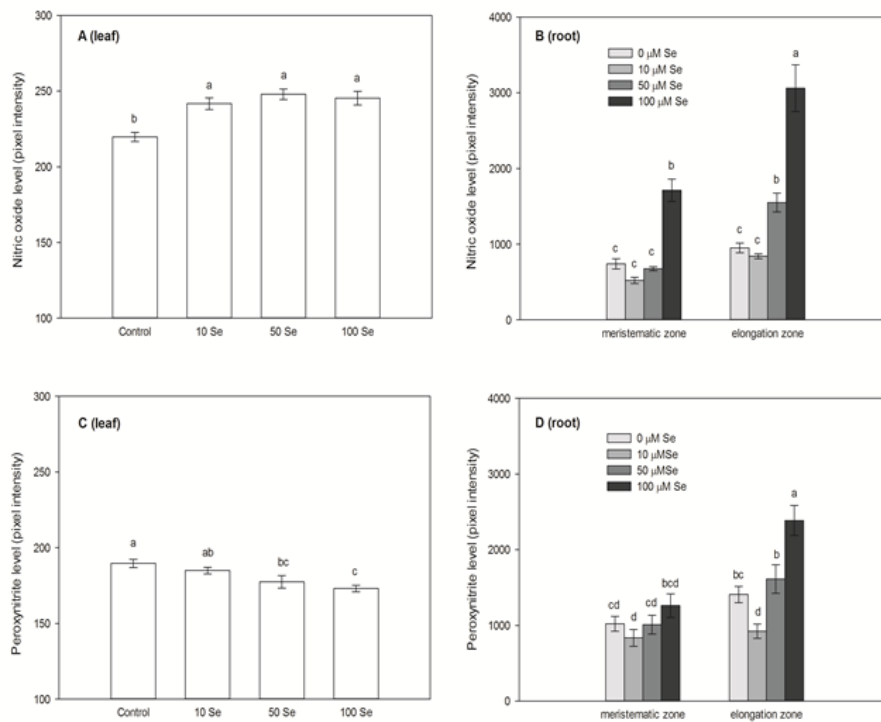
394

395

396 **Selenite differently modified the RNS levels and nitroproteome of pea organs**

397

398         Besides ROS and oxidative stress, the supposed effect of selenite on the formation of  
399 reactive nitrogen species and protein nitration was also evaluated by fluorescent microscopy  
400 and Western blot analysis, respectively. As shown in Fig. 5A, all selenite concentrations  
401 caused a statistically significant but only minor intensification of NO accumulation in the leaf.  
402 Within the root tip, the NO content of the meristem was remarkably enhanced by 100  $\mu$ M,  
403 while in the elongation zone both 50 and 100  $\mu$ M selenite caused NO level increase (Fig. 5B).  
404 Regarding peroxynitrite, treatment with 50 and 100  $\mu$ M selenite significantly decreased its  
405 level in the leaf (Fig. 5C), while only the elongation zone of 100  $\mu$ M selenite-exposed pea  
406 root showed intensified ONOO<sup>-</sup> formation compared to control (Fig. 5D). Furthermore, 10  
407  $\mu$ M selenite led to the significant decrease of peroxynitrite level in the elongation zone, while  
408 in the meristem no changes were detected relative to control level.



409

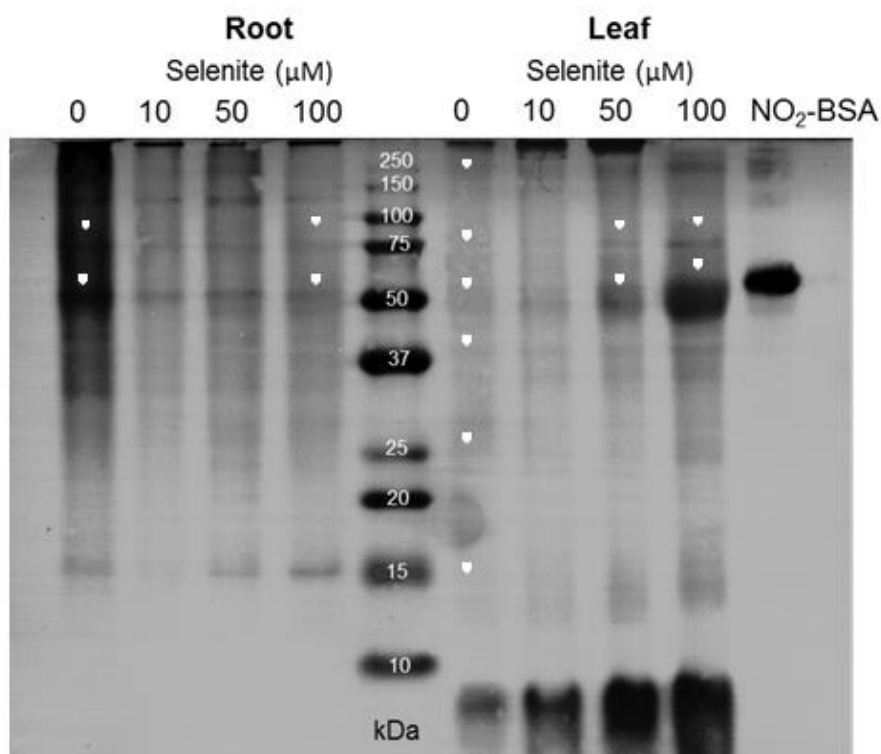
410 **Fig. 5** Nitric oxide (pixel intensity of DAF-FM, AB) and peroxynitrite (pixel intensity of APF, CD) in the leaf  
 411 disks (A and C) and root tips (measured in meristematic and elongation zones, B and D) of control (0) and 10, 50  
 412 or 100  $\mu$ M selenite-exposed pea. Different letters indicate significant differences according to Duncan's test  
 413 ( $n=10$ ,  $P \leq 0.05$ ). (E) Representative fluorescent microscopic images of DAF-FM DA- or APF-stained root tips of  
 414 control and 100  $\mu$ M selenite-treated pea. Bar=0.5 mm

415

416 The RNS-dependent posttranslational modification, protein tyrosine nitration was  
 417 examined by Western blot in the leaf and root of control and selenite-treated pea (Fig. 6). In  
 418 both organs of untreated plants, several 3-nitrotyrosine-positive protein bands were observed.  
 419 In the roots, weakening of the immunoreaction was evident as the effect of selenite. In  
 420 contrast, the protein bands being present also in control leaves (at 200, 75, 50, 37, 25 and 15



421 KDa) showed intensified immunoreaction in case of 50 and 100  $\mu\text{M}$  selenite exposure, while  
422 the lowest applied selenite concentration had no obvious effect on nitration in the leaves.  
423



424  
425 **Fig. 6** Representative immunoblots showing protein tyrosine nitration in the root and leaf system of pea under  
426 control conditions (C) and during 10, 50 or 100  $\mu\text{M}$  selenite exposure. Root and leaf samples were separated by  
427 SDS-PAGE (root: 7.5  $\mu\text{g}$  protein, leaf: 20  $\mu\text{g}$  protein) and analysed by Western blotting with anti-nitrotyrosine  
428 antibody (1:2000). Commercial nitrated BSA (NO<sub>2</sub>-BSA) was used as a positive control. Representative bands  
429 referring to the observed changes are labelled with arrows.

430  
431  
432  
433  
434  
435  
436  
437

## 438 Discussion

439 Pea plants are able to take up selenite from the external medium (Table 1), although  
440 the molecular mechanism of the transport is not well understood. The possibility that selenite  
441 and phosphate may use common membrane transporters was proposed (Haug et al. 2007) and  
442 later confirmed in rice, where the phosphate transporter OsPT2 seems to be greatly involved  
443 in selenite uptake (Zhang et al. 2014). Pea plants showed higher Se accumulation in their root  
444 system compared to the leaves, which was demonstrated by the low leaf:root ratios ranging  
445 from ~0.2 to 0.08. Indeed, selenite was shown to poorly translocate from the root to the shoot  
446 system (Hawrylak-Nowak et al. 2015). It is rather rapidly converted to organic forms  
447 (selenocysteine, selenomethionine, methylselenocysteine), which are retained in the root (de  
448 Souza et al. 1998; Zayed et al. 1998). Based on the tissue concentrations of total selenium  
449 within the leaves, green pea as important forage and crop plant, belongs to the non-  
450 accumulator category (Çakır et al. 2012). Selenium competes with the chemically similar  
451 sulphur during the uptake and assimilation (Hopper and Parker 1999). Therefore, Se in excess  
452 is capable to induce sulphur deficiency response; although Se-exposed pea plants showed  
453 enhanced S contents (Table 1). This can be explained by the fact that excess selenium up-  
454 regulates the expression of sulphate transporters (SULTR1;1 and SULTR2;1) which  
455 consequently lead to S accumulation (Van Hoewyk et al. 2008).

456 The effect of selenite on growth and development of pea proved to be organ- and  
457 concentration-dependent. At the lowest applied concentration, selenite unequivocally  
458 promoted plant growth resulting in extensive growth of plant organs (Fig. 1), which may  
459 enhance fitness. Indeed, there is increasing evidence regarding the beneficial effects of low Se  
460 doses (e.g. 0.5 mg Se L<sup>-1</sup> in soils, 1.0 mg Se L<sup>-1</sup> in hydroponics culture or 1.5 mg Se L<sup>-1</sup> as  
461 foliar spraying) in plants presumably originating from its antioxidant, anti-senescent and  
462 stress-modulator role (Djanaguiraman et al. 2010; Garcia-Banuelos et al. 2011; Kaur et al.  
463 2014; Hawrylak-Nowak et al. 2015). In contrast, selenite at higher doses remarkably  
464 diminished pea growth similarly to other works (reviewed by Kaur et al. 2014). Moreover,  
465 root elongation showed more pronounced Se sensitivity compared to shoot growth, since all  
466 selenite concentrations inhibited it. Also in other species, such as *Arabidopsis thaliana* or  
467 *Brassica napus* root growth was severely reduced by selenite (Tamaoki et al. 2008; Lehotai et  
468 al. 2012; Dimkovikj and Van Hoewyk 2014). One reason for this can be, *inter alia*, the  
469 disturbances in hormone homeostasis (e.g. auxin, cytokinin, ethylene) and cell viability loss of  
470 the primary meristem (Lehotai et al. 2012) and Se-induced alterations in primary metabolism

471 (Dimkovikj and Van Hoewyk 2014). Besides shoot and root growth, selenium exposure in the  
472 form of selenite affected pea development as well, since the higher concentrations of Se (50  
473 and 100  $\mu\text{M}$ ) accelerated the reproductive phase (Fig. 1D). Similarly, reproductive parameters  
474 such as floral bud development, opening of flowers or podding, were induced by 10 and 20  
475  $\mu\text{M}$  selenate in canola (Hajiboland and Keivanfar 2012); although the underlying mechanisms  
476 of Se-triggered flowering are not yet known. Based on these, low selenite concentration  
477 promoted vegetative growth of pea, while severe selenite excess resulted in the inhibition of  
478 growth together with the acceleration of reproductive events. Regarding the pigment  
479 composition of pea leaves (Table 2), the rate of loss was higher in case of chl *a* compared to  
480 chl *b*, which resulted in the reduction of chl *a/b* ratios suggesting that the chl *a* pool is more  
481 sensitive to excess Se than chl *b*. This is contrasting to the results in other plant species such  
482 as spinach or cucumber, where the chl *b* pool was more affected by exogenous selenium  
483 (Hawrylak-Nowak et al. 2015; Saffaryazdi et al. 2012, respectively). By all accounts,  
484 selenium was shown to interact with sulfhydryl containing enzymes such as 5-aminolevulinic  
485 acid dehydratase and porphobilinogen deaminase, resulting in the inhibition of chlorophyll  
486 biosynthesis (Padmaja et al. 1990).

487 Selenium-compounds can evolve pro-oxidant effects disturbing the redox status of  
488 animal and plant cells (Spallholz 1994; Van Hoewyk 2013). Several works concluded that  
489 selenium triggers the formation of ROS. For instance, in the leaves of selenite-exposed  
490 *Arabidopsis* accessions or *Stanleya* species, elevated  $\text{H}_2\text{O}_2$  and superoxide anion levels were  
491 detected (Tamaoki et al. 2008; Freeman et al. 2010) and the root tips of *Arabidopsis* treated  
492 with selenite also showed  $\text{H}_2\text{O}_2$  accumulation (Lehotai et al. 2012). Similarly to these, in both  
493 pea organs, the formation of  $\text{H}_2\text{O}_2$  was induced rather by higher selenite doses (Fig. 2A). Also  
494 at higher concentrations, selenite induced changes in the activities of antioxidant enzymes  
495 such as CAT or APX, and led to lipid peroxidation in the leaves and roots of pea (Fig. 2BCD)  
496 showing correlation to the  $\text{H}_2\text{O}_2$  levels. In e.g. Se-treated barley, lettuce, *Spirulina* and *Ulva*  
497 species the modification of antioxidants and the intensification of lipid peroxidation as the  
498 effect of selenium exposure were reported (Akbulut and Cakir 2010; Ríos et al. 2009; Chen et  
499 al. 2008; Schiavon et al. 2012). One of the major molecules which maintain the cellular redox  
500 homeostasis is glutathione, also having importance in plant growth and development (Gill et  
501 al. 2013). Several studies reported the selenite- or selenate-induced depletion of GSH in both  
502 root and shoot tissues of e.g. *Arabidopsis thaliana*, *Brassica napus*, *Stanleya pinnata* (Van  
503 Hoewyk et al. 2008; Hugouvieux et al. 2009; Tamaoki et al. 2008; Dimkovikj and Van  
504 Hoewyk 2014; Freeman et al. 2010). Similarly, in pea leaves, lower selenite concentrations

505 caused the decrease of total GSH content (Fig. 3A). Although, Dimkovikj and Van Hoewyk  
506 (2014) observed elevated GSH concentration in the whole root system of selenite-exposed  
507 *Brassica* similarly to pea roots in the present study (Fig. 3A). The reason for the selenite-  
508 induced GSH accumulation may partly be the elevation of  $\gamma$ -glutamyl cyclotransferase  
509 (GGCT) protein levels as it was shown in *Brassica* root tissues (Dimkovikj and Van Hoewyk  
510 2014). The remarkable up-regulation of the transcript encoding GGCT2; 1 in the roots of  
511 selenate-exposed *Arabidopsis* (Van Hoewyk et al. 2008) also supports the involvement of this  
512 enzyme in GSH metabolism under Se stress. When the total GSH levels in pea root tips were  
513 examined by fluorescent microscopy, their selenite-triggered reduction was observed (Fig.  
514 3B). The difference between the GSH contents measured by the spectrophotometer and the  
515 fluorescent staining, may simply originate from the technical dissimilarity of the two methods  
516 and suggests that root tips do not represent the whole root system in this case. Similar results  
517 were obtained in the root tips of *Brassica napus* treated with selenite (Dimkovikj and Van  
518 Hoewyk 2014). Since glutathione is associated with auxin transport and is involved in the  
519 maintenance of root growth (Koprivova et al. 2010), its depletion in the root tips may  
520 contribute to the notable inhibition of root elongation found in the present work (see Fig. 1A).  
521 The activity of glutathione S-transferase as a good stress marker was also modified in  
522 selenium-exposed pea plants (Fig. 4AB). From the results obtained for different model  
523 substrates it can be concluded that different GST isoforms are responsible for the pNpa  
524 conjugation after selenite exposure implicating the role of pNpa GST in the detoxification  
525 during selenite exposure in pea. The involvement of GST in selenium stress response is  
526 supported by the strong up-regulation of GST gene (At2g02390) in selenate-treated  
527 *Arabidopsis* (Van Hoewyk et al. 2008) or *Stanleya* species (GSTF6, Freeman et al. 2010).  
528 Glutathione reductase enzyme maintains the reduced status of GSH and acts as a substrate for  
529 glutathione S-transferases (Yousuf et al. 2012). The lowest applied selenium concentration  
530 dramatically induced GR activity in the root (Fig. 4C) consequently helping to maintain the  
531 level of reduced GSH, which in turn can be used as a substrate for GSTs during defence  
532 mechanisms. Also in coffee cell suspension, selenite at low concentration was able to notably  
533 increase GR activity (Gomes-Junior et al. 2007). In the leaves, GR activity also elevated as  
534 the result of selenite exposure suggesting the key role of this enzyme in selenite tolerance.  
535 Alternatively, high reduced GSH content may also be used for selenite reduction to  
536 selenodiglutathione similarly to animal systems (Wallenberg et al. 2010), although molecular  
537 evidence for GR being a rate limiting enzyme in Se metabolism of plants is still lacking  
538 (Terry et al. 2000). Consequently, our results confirm the occurrence of selenium-induced

539 oxidative stress, though this depends on the concentration of Se. As it was suggested by  
540 Hartikainen et al. (2000), at low concentration (in this study 10  $\mu\text{M}$ ) Se has promoting effect  
541 on growth and does not induce oxidative stress, while at higher doses (here 50 and 100  $\mu\text{M}$ ) it  
542 triggers oxidative stress and deteriorates pea growth. Moreover, our results confirm that  
543 glutathione and related enzymes play a crucial role in selenium stress responses.

544 Besides ROS, the effect of selenite on RNS levels was also monitored and intensive  
545 NO generation was observed in the root tips of treated plants (Fig. 5B). The most significant  
546 and concentration-dependent selenite-triggered NO formation was detected in the elongation  
547 zone of root tips suggesting the tissue specificity of this response. Selenite presumably  
548 induces the main NO synthesizing enzyme of the root; nitrate reductase, as it was reported in  
549 lettuce (Ríos et al. 2010). Moreover, also in the leaves NR may be the source of selenite-  
550 triggered NO (Fig. 5A), since it can contribute to NO synthesis in the aerial plant parts as well  
551 (Zhang et al. 2011; Zhao et al. 2009). The effect of selenium on NR can be direct or indirect,  
552 since Se-induced S deficiency may increase molybdenum content thus inducing NR  
553 (Shinmachi et al. 2010; Yu et al. 2010). Being a highly oxidative and nitrosative agent  
554 (Arasimowicz-Jelonek and Floryszak-Wieczorek 2011), peroxy nitrite diminution in leaves  
555 and roots as the effect of low selenite doses suggests that selenite at low concentration would  
556 activate some peroxy nitrite detoxification mechanisms. In the leaf, also more severe selenium  
557 exposure reduced peroxy nitrite levels reflecting a more efficient detoxification in this organ.  
558 One possibility of peroxy nitrite scavenging is the reaction of it with glutathione leading to the  
559 formation of S-nitrosoglutathione and NO (Arasimowicz-Jelonek and Floryszak-Wieczorek  
560 2011). The high GSH content in the selenium-exposed pea together with the NO accumulation  
561 may reflect to this ONOO<sup>-</sup> detoxification pathway. Additionally, key enzymes in the  
562 decomposition of ONOO<sup>-</sup> are the glutathione peroxidases and thioredoxin reductases. In  
563 animals and humans, these enzymes contain selenocystein (SeCys) being essential for their  
564 catalytic activity (Schrauzer 2000). Although, there is no evidence regarding the incorporation  
565 of SeCys in proteins in plants, thus the role of selenium in the regulation of enzyme activity in  
566 plants is still unknown (Van Hoewyk 2013).

567 Protein tyrosine nitration as an RNS-dependent posttranslational modification  
568 contributes to the evolution of the secondary nitrosative stress. Investigating this  
569 posttranslational modification of proteins by Western blot (Fig. 6), it was observed that this  
570 PTM being present in unstressed pea plants is a basal mechanism of the regulation of protein  
571 activity in green pea. In pea and in other plant species, such as sunflower and pepper nitration

572 was observed during control circumstances by others (Corpas et al. 2009; Chaki et al. 2009;  
573 2015). Furthermore, as in the work of Corpas et al. (2009) the root proteome of pea proved to  
574 be more nitrated compared to that of the leaf, which reflects the organ-specific nature of  
575 tyrosine nitration. Besides, the organs differentially responded to selenite exposure. In the root  
576 system, the nitration pattern of the proteome was not modified, since new nitrated protein  
577 bands were not observed. In contrast, the nitration level of leaf proteome was significantly  
578 intensified by selenite similarly to; *inter alia*, salt-stressed olive leaves, cold-treated pea  
579 leaves or arsenic-exposed *Arabidopsis* (reviewed in Corpas et al. 2013). In the leaves of pea,  
580 the level of nitration well correlated with the exogenous selenite concentrations suggesting the  
581 concentration-dependent feature of protein tyrosine nitration. At the same time, modifications  
582 of the nitroproteome show no strict correlation to the alterations in the NO and ONOO<sup>-</sup> levels  
583 which partly can be the reason of the high reactivity of these forms with each other and with  
584 other molecules. Also, it is worth mentioning that the nitrogen dioxide radical (NO<sub>2</sub><sup>·</sup>) also  
585 possesses a notable nitrating capacity, thus the amount of this molecule may determine the  
586 rate of nitration as well (Souza et al. 2008).

587 Altogether, selenite alters vegetative and reproductive development of pea. At low  
588 dose, it promotes growth and does not disturb the cellular ROS and RNS metabolism.  
589 Moreover, our results confirmed that severe selenite stress inhibits growth and concomitantly  
590 induces oxidative stress. Besides, the presented data first reveals selenite-induced  
591 concentration- and organ-dependent nitrosative stress in pea. Since oxidative and nitrosative  
592 mechanisms occur in parallel, we urge to consider nitro-oxidative stress as an underlying  
593 mechanism of selenium phytotoxicity.

594

595

596

597 **Acknowledgement** This research was supported and co-financed by the European  
598 Cooperation in Science and Technology (COST) Short-Term Scientific Mission in the  
599 framework of COST Action FA 0905 – Mineral Improved Crop Production for Healthy Food  
600 and Feed (reference code COST-STSM-ECOST-STSM-FA0905-010212-013321). Authors  
601 also acknowledge TÁMOP-4.2.2.B-15/1/KONV-2015-0006 project for supporting the  
602 experiments. The infrastructural background and the purchasing of consumables were ensured  
603 by the Hungarian Scientific Research Fund (Grant no. OTKA PD100504) and the Hungary-  
604 Serbia IPA Cross-border Co-operation Programme (PLANTTRAIN, HUSRB/1203/221/173).

605

606 **References**

607

608 Akbulut M, Çakır S (2010) The effects of Se phytotoxicity on the antioxidant systems of leaf  
609 tissues in barley (*Hordeum vulgare* L.) seedlings. *Plant Phys Biochem* 48: 160–166

610 Arasimowicz-Jelonek M, Floryszak-Wieczorek J (2011) Understanding the fate of  
611 peroxyxynitrite in plant cells – From physiology to pathophysiology. *Phytochem* 72:681-  
612 688

613 Bradford MM (1976) A rapid and sensitive method for the quantification of microgram  
614 quantities of protein utilizing the principle of protein-dye-binding. *Anal Biochem*  
615 72:248-255

616 Çakır Ö, Turgut-Kara N and Arı Ş (2012) Selenium Metabolism in Plants: Molecular  
617 Approaches. In: Montanaro G, Dichio B (eds) *Advances in Selected Plant Physiology*  
618 *Aspects* InTech, Croatia ISBN: 978-953- 51-0557-2 doi:10.5772/32770, available  
619 from: [http://www.intechopen.com/books/advances-in-selected-plant-](http://www.intechopen.com/books/advances-in-selected-plant-physiologyaspects/selenium-metabolism-in-plants-molecular-approaches)  
620 [physiologyaspects/selenium-metabolism-in-plants-molecular-approaches](http://www.intechopen.com/books/advances-in-selected-plant-physiologyaspects/selenium-metabolism-in-plants-molecular-approaches)

621 Chaki M, de Morales PÁ, Ruiz C, Begara-Morales JC, Barroso JB, Corpas FJ, Palma JM  
622 (2015) Ripening of pepper (*Capsicum annuum*) fruit is characterized by an  
623 enhancement of protein tyrosine nitration. *Ann Bot* doi:10.1093/aob/mcv016

624 Chaki M, Valderrama R, Fernández-Ocana AM et al (2009) Protein targets of tyrosine  
625 nitration in sunflower (*Helianthus annuus* L.) hypocotyls. *J Exp Bot* 60:4221-4234

626 Chen TF, Zheng WJ, Wong YS, Yang F (2008) Selenium-induced changes in activities of  
627 antioxidant enzymes and content of photosynthetic pigments in *Spirulina platensis*. *J*  
628 *Integr Plant Biol* 50: 40–48

629 Corpas FJ and Barroso JB (2013) Nitro-oxidative stress vs oxidative or nitrosative stress in  
630 higher plants. *New Phytol* 199:633-635

631 Corpas FJ, Barroso JB, Carreras A, Valderrama R, Palma JM, del Río LA (2007) Nitrosative  
632 stress in plants: A new approach to understand the role of NO in abiotic stress. In:  
633 *Nitric Oxide in Plant Growth, Development and Stress Physiology*. *Plant Cell Monogr*,  
634 Springer Berlin Heidelberg, 5: 187-205

635 Corpas FJ, Chaki M, Fernández- Ocaña A, Valderrama R, Palma JM, Carreras A, Begara-  
636 Morales JC, Airaki M, del Río LA, Barroso JB (2008) Metabolism of Reactive  
637 Nitrogen Species in Pea Plants Under Abiotic Stress Conditions. *Plant Cell Phys*  
638 49:1711-1722

639 Corpas FJ, Chaki M, Leterrier M, Barroso JB (2009) Protein tyrosine nitration: a new  
640 challenge in plants. *Plant Sign Behav* 4:920-923

641 Corpas FJ, Leterrier M, Valderrama R, Airaki M, Chaki M, Palma JM, Barroso JB (2011)  
642 Nitric oxide imbalance provokes a nitrosative response in plants under abiotic stress.  
643 *Plant Sci* 181:604-611

644 Corpas FJ, Palma JM, del Río LA, Barroso JB (2013) Protein tyrosine nitration in higher  
645 plants grown under natural and stress conditions. *Front Plant Sci* 4:29, doi:  
646 10.3389/fpls.2013.00029

647 de Souza MP, Pilon-Smits EAH, Lytle CM, Hwang S, Tai J, Honma TSU, Yeh L, Terry N  
648 (1998) Rate-limiting steps in selenium assimilation and volatilization by Indian  
649 mustard. *Plant Phys* 117: 1487-1494

650 Dhillon KS and Dhillon SK (2003) Distribution and management of seleniferous soils. *Adv*  
651 *Agr* 79:119–184

652 Dhillon SK, Dhillon KS, Kohli A, Khera KL (2008) Evaluation of leaching and runoff losses  
653 of selenium from seleniferous soils through simulated rainfall. *J Plant Nutr Soil*  
654 171:187 – 192

655 Dimkovikj A and Van Hoewyk D (2014) Selenite activates the alternative oxidase pathway  
656 and alters primary metabolism in *Brassica napus* roots: evidence of a mitochondrial  
657 stress response. *BMC Plant Biol* 14:259. doi:10.1186/s12870-014-0259-6

658 Djanaguiraman M, Prasad PV, Seppanen M (2010) Selenium protects sorghum leaves from  
659 oxidative damage under high temperature stress by enhancing antioxidant defense  
660 system. *Plant Physiol Biochem* 48:999–1007. doi:10.1016/j.plaphy.2010.09.009

661 Freeman JL, Tamaoki M, Stushnoff C et al (2010) Molecular mechanisms of selenium  
662 tolerance and hyperaccumulation in *Stanleya pinnata*. *Plant Phys* 153: 1630–1652

663 Galetskiy D, Lohscheider JN, Kononikhin AS, Popov IA, Nikolaev EN, Adamska I (2011)  
664 Mass spectrometric characterization of photooxidative protein modifications in  
665 *Arabidopsis thaliana* thylakoid membranes. *Rap Comm Mass Spectr* 25:184-190

666 Garcia-Banuelos ML, Hermosillo-Cereceres A, Sanchez EM (2011) The Importance of  
667 Selenium Biofortification in Food Crops. *Curr Nutr Food Sci*, 7:181-190

668 Gill SS, Anjum NA, Hasanuzzaman M, Gill R, Kumar DT, Ahmad I, Pereira E, Tuteja N  
669 (2013) Glutathione and glutathione reductase: A boon in disguise for plant abiotic  
670 stress defense operations. *Plant Phys Biochem* 70:204-212



671 Gomes-Junior RA, Gratão PL, Gaziola SA, Mazzafera P, Lea PJ, Azevedo RA (2007)  
672 Selenium-induced oxidative stress in coffee cell suspension cultures. *Funct Plant Biol*  
673 34:449–456

674 Grant K, Carey NM, Mendoza M, Schulze J, Pilon M, Pilon-Smits EAH, Van Hoewyk D  
675 (2011) Adenosine 5'-phosphosulphate reductase (APR2) mutation in *Arabidopsis*  
676 implicates glutathione deficiency in selenite toxicity. *Biochem J* 438: 325-335

677 Griffith OW (1980) Determination of glutathione and glutathione disulfide using glutathione  
678 reductase and 2-vinylpyridine. *Anal Biochem* 106:207-211

679 Guan ZQ, Chai TY, Zhang YX, Xu J, Wei W (2009) Enhancement of Cd tolerance in  
680 transgenic tobacco overexpressing a Cd-induced catalase cDNA. *Chemosphere*  
681 76:623–630

682 Hajiboland R and Keivanfar N (2012) Selenium supplementation stimulates vegetative and  
683 reproductive growth in canola (*Brassica napus* L.) plants. *Acta Agric Sloven*  
684 doi:10.2478/v10014-012-0002-7

685 Hartikainen H, Xue T, Piironen V (2000) Selenium as an antioxidant and pro-oxidant in  
686 ryegrass. *Plant Soil* 225:193–200. doi:10.1023/A:1026512921026

687 Haug A, Graham RD, Christophersen OA, Lyons GH (2007) How to use the world's scarce  
688 selenium resources efficiently to increase the selenium concentration in food. *Microb*  
689 *Ecol Health Dis* 19:209-228

690 Hawrylak-Nowak B, Matraszek R, Pogorzelec M (2015) The dual effects of two inorganic  
691 selenium forms on the growth, selected physiological parameters and macronutrients  
692 accumulation in cucumber plants. *Acta Physiol Plant* DOI 10.1007/s11738-015-1788-9

693 Heath RL, Packer L (1968) Photoperoxidation in isolated chloroplasts. I. Kinetics and  
694 stoichiometry of fatty acid peroxidation. *Arch Biochem Biophys* 125:180-198

695 Hopper JL, Parker DR (1999) Plant availability of selenite and selenate as influenced by the  
696 competing ions phosphate and sulfate. *Plant Soil* 210: 199–207

697 Hugouvieux V, Dutilleul C, Jourdain A, Reynaud F, Lopez V, Bourguignon J (2009)  
698 *Arabidopsis* putative selenium-binding protein1 expression is tightly linked to cellular  
699 sulfur demand and can reduce sensitivity to stresses requiring glutathione for  
700 tolerance. *Plant Phys* 151:768-81

701 Kaur N, Sharma S, Kaur S, Nayyar H (2014) Selenium in agriculture: a nutrient or  
702 contaminant for crops? *Arch Agr Soil Sci*, 60:12, 1593-1624, doi:  
703 10.1080/03650340.2014.918258

704 Kolbert Zs, Petó A, Lehotai N, Feigl G, Ördög A, Erdei L (2012) *In vivo* and *in vitro* studies  
705 on fluorophore-specificity. *Acta Biol Szeged* 56:37–41

706 Koprivova A, Mugford ST, Kopriva S (2010) *Arabidopsis* root growth dependence on  
707 glutathione is linked to auxin transport. *Plant Cell Reports* 29:1157–1167

708 Lehotai N, Kolbert Zs, Petó A, Feigl G, Ördög A, Kumar D, Tari I, Erdei L (2012) Selenite-  
709 induced hormonal and signaling mechanisms during root growth of *Arabidopsis*  
710 *thaliana* L.. *J Exp Bot* 63:5677–5687

711 Lehotai N, Petó A, Erdei L, Kolbert Zs (2011) The effect of selenium (Se) on development  
712 and nitric oxide levels in *Arabidopsis thaliana* seedlings. *Acta Biol Szeged* 55: 105-  
713 107

714 Lichtenthaler HK (1987) Chlorophylls and Carotenoids: Pigments of  
715 photosynthetic membranes. *Meth Enzym* 148:350-382

716 Lindermayr C and Durner J (2015) Interplay of Reactive Oxygen Species and Nitric Oxide:  
717 Nitric Oxide Coordinates Reactive Oxygen Species Homeostasis. *Plant Phys*  
718 167:1209-1210

719 Mengel K, Kirkby EA (1987) Principles of plant nutrition. International Potash Institute,  
720 Bern, Switzerland 62-66.

721 Ohno M, Uraji M, Shimoishi Y, Mori IC, Nakamura Y, Murata Y (2012) Mechanisms of the  
722 Selenium Tolerance of the *Arabidopsis thaliana* Knockout Mutant of Sulfate  
723 Transporter SULTR1;2. *Biosci Biotech Biochem* 76:993-998

724 Padmaja K, Prasad DD, Prasad AR (1990) Selenium as a novel regulator of porphyrin  
725 biosynthesis in germinating seedlings of mung bean (*Phaseolus vulgaris*). *Biochem*  
726 *Internat* 22:441-446

727 Procházková D, Sumaira J, Wilhelmová N, Pavlíková D, Száková J (2014) Chapter 11 -  
728 Reactive Nitrogen Species and the Role of NO in Abiotic Stress. In: P. Ahmad (Ed):  
729 Emerging Technologies and Management of Crop Stress Tolerance: A Sustainable  
730 Approach. Academic Press 2:249-266

731 Reilly C (1996) Selenium. In: Chapman E, Hall W (eds) Selenium in food and health. Blackie  
732 Academic & Professional, London, p 1–24

733 Ríos JJ, Blasco B, Cervilla LM, Rosales MA, Sanchez-Rodriguez E, Romero L, Ruiz JM  
734 (2009) Production and detoxification of H<sub>2</sub>O<sub>2</sub> in lettuce plants exposed to selenium.  
735 *Ann Appl Biol* 154:107–116

736 Ríos JJ, Blasco B, Rosales MA, Sanchez-Rodriguez E, Leyva R, Cervilla LM, Romero L,  
737 Ruiz JM (2010) Response of nitrogen metabolism in lettuce plants subjected to  
738 different doses and forms of selenium. *J Sci Food Agric* 90:1914-1919

739 Saffaryazdi A, Lahouti M, Ganjeali A, Bayat H (2012) Impact of selenium supplementation  
740 on growth and selenium accumulation on spinach (*Spinacia oleracea* L.) plants. *Not*  
741 *Sci Biol* 4:95–100

742 Santalla M, Amurrio JM, De Ron AM (2001) Food and feed potential breeding value of  
743 green, dry and vegetable pea germplasm. *Can J Plant Sci* 81:601-610

744 Schiavon M, Moro I, Pilon-Smit EAH, Matozzo V, Malagoli M, Vecchia FD (2012)  
745 Accumulation of selenium in *Ulva* sp. and effects on morphology, ultrastructure and  
746 antioxidant enzymes and metabolites. *Aqua Toxic* 122: 222–231

747 Schrauzer GN (2000) Selenomethionine: A review of its nutritional significance, metabolism  
748 and toxicity. *JN Nutr* 130:1653-1656

749 Schröder P, Meier H, Debus R (2005) Detoxification of Herbicides in *Phragmites australis*. *Z*  
750 *Naturforsch* 60c:317-324

751 Shinmachi F, Buchner P, Stroud LJ, Parmar S, Zhao F-J, McGrath SP, Hawkesford MJ (2010)  
752 Influence of sulphur deficiency on the expression of specific sulphate transporters and  
753 the distribution of sulphur, selenium, and molybdenum in wheat. *Plant Phys* 153: 327-  
754 336

755 Souza JM, Peluffo G, Radi R (2008) Protein tyrosine nitration. Functional alteration or just a  
756 biomarker? *Free Rad Biol Med* 45:357-366

757 Spallholz JE (1994) On the nature of selenium toxicity and carcinostatic activity. *Free Radical*  
758 *Biol Med* 17: 45–64

759 Tamaoki M, Freeman JL, Pilon-Smits EAH (2008) Cooperative ethylene and jasmonic acid  
760 signaling regulates selenate resistance in *Arabidopsis*. *Plant Phys* 146: 1219–1230

761 Tripathi N, Misra SG (1974) Uptake of applied selenium by plants. *Indian J Agric Sci* 44:804-  
762 807

763 Terry N, Zayed A, de Souza P, Tarun A (2000) Selenium in higher plants. *Ann Rev Plant*  
764 *Phys Plant Mol Biol* 51:401–432

765 Van der Vliet A, Eiserich JP, Shigenana MK, Cross CE (1999) Reactive nitrogen species and  
766 tyrosine nitration in the respiratory tract: epiphenomena or a pathobiologic mechanism  
767 of disease? *Am J Respir Crit Care Med* 160:1-9

768 Van Hoewyk D (2013) A tale of two toxicities: malformed selenoproteins and oxidative stress  
769 both contribute to selenium stress in plants. *Ann Bot* 112:965-72

770 Van Hoewyk D, Takahashi H, Inoue E, Hess A, Tamaoki M, Pilon-Smits EAH (2008)  
771 Transcriptome analyses give insights into selenium-stress responses and selenium  
772 tolerance mechanisms in *Arabidopsis*. *Phys Plant* 132: 236-253

773 Vanacker H, Carver TLW, Foyer CH (1998) Pathogen-induced changes in the antioxidant  
774 status of the apoplast in barley leaves. *Plant Phys* 117:1103-1114

775 Velikova V, Yordanov I, Edreva A (2000) Oxidative stress and some antioxidant systems in  
776 acid rain-treated bean plants. Protective role of exogenous polyamines. *Plant Sci*  
777 151:59-66

778 Verma S, Dubey RS (2003) Lead toxicity induces lipid peroxidation and alters the activities  
779 of antioxidant enzymes in growing rice plants. *Plant Sci* 164:645-655

780 Wallenberg M, Olm E, Hebert C, Björnstedt M, Fernandes AP (2010) Selenium compounds  
781 are substrates for glutaredoxins: a novel pathway for selenium metabolism and a  
782 potential mechanism for selenium-mediated cytotoxicity. *Biochem J* 429: 85–93

783 Wang Y, Loake GJ, Chu C (2013) Cross-talk of nitric oxide and reactive oxygen species in  
784 plant programmed cell death. *Front Plant Sci* 4:1-7

785 Yousuf PY, Hakeem KUR, Chandna R, Ahmad P (2012) Role of Glutathione Reductase in  
786 Plant Abiotic Stress. In: Ahmad P and Prasad MNV (eds.) *Abiotic Stress Responses in*  
787 *Plants: Metabolism, Productivity and Sustainability*. Doi:10.1007/978-1-4614-0634-  
788 1\_8 Springer, Netherlands

789 Yu R, Kampschreur MJ, van Loosdrecht MCM, Chandran K (2010) Mechanisms and specific  
790 directionality of autotrophic nitrous oxide and nitric oxide generation during transient  
791 anoxia. *Environ Sci Tech* 44:1313-1319

792 Zayed A, Lytle CM, Terry N (1998) Accumulation and volatilization of different chemical  
793 species of selenium by plants. *Planta* 206:284-292

794 Zhang J, Kirkham MB (1996) Antioxidant responses to drought in sunflower and sorghum  
795 seedlings. *New Phytol* 132:361-373

796 Zhang L, Hu B, Li W et al (2014) OsPT2, a phosphate transporter, is involved in the active  
797 uptake of selenite in rice. *New Phytol* 201:1183-1191

798 Zhang M, Dong J-F, Jin H-H, Sun L-N, Xu M-J (2011) Ultraviolet-B-induced flavonoid  
799 accumulation in *Betula pendula* leaves is dependent upon nitrate reductase-mediated  
800 nitric oxide signalling. *Tree Phys* 31:798-807

801 Zhao M-G, Chen L, Zhang L-L, Zhang W-H (2009) Nitric reductase-dependent nitric oxide  
802 production is involved in cold acclimation and freezing tolerance in *Arabidopsis*. *Plant*  
803 *Phys* 151:755-767

804 **Figure legends**

805

806 **Table 1** Total selenium (Se) and sulphur (S) concentrations ( $\mu\text{g/g}$  dry weight) in the leaves  
807 and roots of pea plants treated with 0, 10, 50 or 100  $\mu\text{M}$  selenite. Leaf:root ratios of Se  
808 concentrations in control and selenite-treated pea plants. Different letters indicate significant  
809 differences according to Duncan's test ( $n=6$ ,  $P\leq 0.05$ )

810 **Fig. 1** The length (cm, A) and the fresh weight (g, B) of the shoot and root system of pea  
811 plants treated with 0, 10, 50, 100  $\mu\text{M}$  selenite. Different letters indicate significant differences  
812 according to Duncan's test ( $n=6$ ,  $P\leq 0.05$ ). (C) Representative photographs showing the shoot  
813 and root system of control (0  $\mu\text{M}$  Se) and Se-treated pea plants. Bar=5 cm. (D) Representative  
814 photographs showing the shoot system of control (0  $\mu\text{M}$  Se), 50 or 100  $\mu\text{M}$  Se-exposed pea.  
815 White arrows indicate flowers appeared as the effect of the treatments. Bar=10 cm

816 **Table 2** Concentrations of photosynthetic pigments ( $\mu\text{g/g}$  fresh weight) and the chlorophyll  
817 a/b ratios in the leaves of control and selenite-treated pea plants. Different letters indicate  
818 significant differences according to Duncan's test ( $n=6$ ,  $P\leq 0.05$ )

819 **Fig. 2** Hydrogen peroxide concentration in pea leaves and root, measured  
820 spectrophotometrically (A) and detected by DAB staining (a) in the leaves of pea (from left:  
821 control, 10, 50 and 100  $\mu\text{M}$  Se, Bar=1 cm). Activity ( $\mu\text{kat/mg}$  protein) of ascorbate  
822 peroxidase (B) and catalase (C) in the leaves and roots of pea. (D) The concentration of  
823 TBARS in the leaf and root of pea plants treated with 0, 10, 50, 100  $\mu\text{M}$  selenite. Different  
824 letters indicate significant differences according to Duncan's test ( $n=6$ ,  $P\leq 0.05$ )

825 **Fig. 3** (A) Concentration of total glutathione ( $\mu\text{mol/g}$  fresh weight) in the leaves and roots of  
826 control and selenite-exposed pea. Different letters indicate significant differences according to  
827 Duncan's test ( $n=6$ ,  $P\leq 0.05$ ). (B) Representative microscopic images of MBB-stained root tips  
828 of control (0  $\mu\text{M}$  Se) and 10, 50, 100  $\mu\text{M}$  selenite-treated pea. Bar=100  $\mu\text{m}$ . (b)  
829 Representative microscopic images of MBB-stained root tips treated with water (Control), 1  
830 mM GSH or 10 mM CDNB. Bar=100  $\mu\text{m}$

831 **Fig. 4** Specific activity ( $\mu\text{kat/ mg}$  protein) of glutathione-S-transferase in control and 10, 50 or  
832 100  $\mu\text{M}$  selenite-treated pea leaves (A) and root (B) determined by using the model substrates  
833 CDNB, fluorodifen, pNpa and NBC. (C) Specific activity ( $\mu\text{kat/ mg}$  protein) of glutathione  
834 reductase in the leaves and roots of pea treated with 0, 10, 50 or 100  $\mu\text{M}$  Se. Different letters  
835 indicate significant differences according to Duncan's test ( $n=5$ ,  $P\leq 0.05$ )

836 **Fig. 5** Nitric oxide (pixel intensity of DAF-FM, AB) and peroxyntirite (pixel intensity of  
837 APF, CD) in the leaf disks (A and C) and root tips (measured in meristematic and elongation

838 zones, B and D) of control (0) and 10, 50 or 100  $\mu\text{M}$  selenite-exposed pea. Different letters  
839 indicate significant differences according to Duncan's test ( $n=10$ ,  $P\leq 0.05$ ). (E) Representative  
840 fluorescent microscopic images of DAF-FM DA- or APF-stained root tips of control and 100  
841  $\mu\text{M}$  selenite-treated pea. Bar=0.5 mm

842 **Fig. 6** Representative immunoblots showing protein tyrosine nitration in the root and leaf  
843 system of pea under control conditions (C) and during 10, 50 or 100  $\mu\text{M}$  selenite exposure.  
844 Root and leaf samples were separated by SDS-PAGE (root: 7.5  $\mu\text{g}$  protein, leaf: 20  $\mu\text{g}$   
845 protein) and analysed by Western blotting with anti-nitrotyrosine antibody (1:2000).  
846 Commercial nitrated BSA ( $\text{NO}_2\text{-BSA}$ ) was used as a positive control. Representative bands  
847 referring to the observed changes are labelled with arrows.